

Circulation

JOURNAL OF THE AMERICAN HEART ASSOCIATION



Disruption of the Cathepsin K Gene Reduces Atherosclerosis Progression and Induces Plaque Fibrosis but Accelerates Macrophage Foam Cell Formation

E. Lutgens, S.P.M. Lutgens, B.C.G. Faber, S. Heeneman, M.M.J. Gijbels, M.P.J. de Winther, P. Frederik, I. van der Made, A. Daugherty, A.M. Sijbers, A. Fisher, C.J. Long, P. Saftig, D. Black, M.J.A.P. Daemen and K.B.J.M. Cletjens

Circulation 2006;113:98-107; originally published online Dec 19, 2005;

DOI: 10.1161/CIRCULATIONAHA.105.561449

Circulation is published by the American Heart Association, 7272 Greenville Avenue, Dallas, TX 75214

Copyright © 2006 American Heart Association. All rights reserved. Print ISSN: 0009-7322. Online ISSN: 1524-4539

The online version of this article, along with updated information and services, is located on the World Wide Web at:

<http://circ.ahajournals.org/cgi/content/full/113/1/98>

Subscriptions: Information about subscribing to *Circulation* is online at
<http://circ.ahajournals.org/subscriptions/>

Permissions: Permissions & Rights Desk, Lippincott Williams & Wilkins, 351 West Camden Street, Baltimore, MD 21202-2436. Phone 410-5280-4050. Fax: 410-528-8550. Email:
journalpermissions@lww.com

Reprints: Information about reprints can be found online at
<http://www.lww.com/static/html/reprints.html>

Disruption of the *Cathepsin K* Gene Reduces Atherosclerosis Progression and Induces Plaque Fibrosis but Accelerates Macrophage Foam Cell Formation

E. Lutgens, MD, PhD*; S.P.M. Lutgens, MSc*; B.C.G. Faber, PhD; S. Heeneman, PhD; M.M.J. Gijbels, PhD; M.P.J. de Winther, PhD; P. Frederik, PhD; I. van der Made, MSc; A. Daugherty, PhD; A.M. Sijbers, PhD; A. Fisher, PhD; C.J. Long, PhD; P. Saftig, PhD; D. Black, PhD; M.J.A.P. Daemen, MD, PhD; K.B.J.M. Cleutjens, PhD

Background—Cathepsin K (catK), a lysosomal cysteine protease, was identified in a gene-profiling experiment that compared human early plaques, advanced stable plaques, and advanced atherosclerotic plaques containing a thrombus, where it was highly upregulated in advanced stable plaques.

Methods and Results—To assess the function of catK in atherosclerosis, catK^{-/-}/apolipoprotein (apo) E^{-/-} mice were generated. At 26 weeks of age, plaque area in the catK^{-/-}/apoE^{-/-} mice was reduced (41.8%) owing to a decrease in the number of advanced lesions as well as a decrease in individual advanced plaque area. This suggests an important role for catK in atherosclerosis progression. Advanced plaques of catK^{-/-}/apoE^{-/-} mice showed an increase in collagen content. Medial elastin fibers were less prone to rupture than those of apoE^{-/-} mice. Although the relative macrophage content did not differ, individual macrophage size increased. In vitro studies of bone marrow derived-macrophages confirmed this observation. Scavenger receptor-mediated uptake (particularly by CD36) of modified LDL increased in the absence of catK, resulting in an increased macrophage size because of increased cellular storage of cholesterol esters, thereby enlarging the lysosomes.

Conclusions—A deficiency of catK reduces plaque progression and induces plaque fibrosis but aggravates macrophage foam cell formation in atherosclerosis. (*Circulation*. 2006;113:98-107.)

Key Words: atherosclerosis ■ lipids ■ pathology ■ proteases ■ cathepsins

Proteases have been linked to the cascade of pathological alterations involved in atherosclerosis. The lysosomal cysteine proteases, or cathepsins,¹ recently received much interest in the vascular field.² Large-scale gene-expression studies indicated differential expression of cathepsin B, L, S, and H mRNAs in atherosclerotic human and mouse arteries.³⁻⁶ Cathepsin S, D, F, K, L, and V proteins⁷⁻¹⁰ were present in human atheromata. Interestingly, cysteine proteases account for 40% of the total elastase activity of human atheroma extracts.⁷

Clinical Perspective p 107

Genetic disruption of the cathepsin S gene reduced plaque progression in LDL receptor-deficient mice¹¹ and inhibited angiogenesis.¹² Cathepsin L is required for endothelial pro-

genitor cell-induced neovascularization.¹³ In addition, a decrease in cystatin C levels, the most abundant extracellular inhibitor of cysteine proteases,¹⁴ was frequently observed in patients with severe vascular disease.¹⁵ Apolipoprotein (apo) E^{-/-} mice deficient in cystatin C developed atherosclerotic plaques that were rich in collagen and smooth muscle cells (SMCs) and developed progressive aortic dilatation.¹⁶ These data indicate an important role for cathepsins in plaque progression.

In a recent suppressive subtractive hybridization analysis of whole-mount human atherosclerotic plaques that compared stable atherosclerotic plaques and plaques containing thrombus, we identified upregulation of cathepsin K (catK) in advanced stable plaques.¹⁷ catK is composed of a 15-residue N-terminal signal peptide, a 99-residue propeptide, and a

Received May 22, 2005; revision received September 25, 2005; accepted October 20, 2005.

From the Departments of Pathology (E.L., S.P.M.L., B.C.G.F., S.H., M.M.J.G., M.J.A.P.D., K.B.J.M.C.), Molecular Genetics (M.M.J.G., M.P.J.d.W., I.v.d.M.), and Electron Microscopy (P.F.), Cardiovascular Research Institute Maastricht, University of Maastricht, Maastricht, the Netherlands; the University of Kentucky (A.D.), Lexington; Organon Scotland (A.M.S., A.F., C.J.L., D.B.), Newhouse, Scotland; and the Biochemical Institute (P.S.), University of Kiel, Kiel, Germany.

*The first 2 authors contributed equally to this work.

The online-only Data Supplement can be found with this article at <http://circ.ahajournals.org/cgi/content/full/CIRCULATIONAHA.105.561449/DC1>.

Correspondence to E. Lutgens, MD, PhD, Department of Pathology, Cardiovascular Research Institute Maastricht, University of Maastricht, PO Box 616, 6200 MD Maastricht, The Netherlands. E-mail E.Lutgens@path.unimaas.nl

© 2006 American Heart Association, Inc.

Circulation is available at <http://www.circulationaha.org>

DOI: 10.1161/CIRCULATIONAHA.105.561449

mature protein of 215 amino acids. catK is the most potent mammalian elastase yet described and harbors unique collagenolytic activity.^{18,19} catK was originally identified in an osteoclast cDNA library, but it has since been found to be expressed in many tissues, such as arteries, breast, ovary, stomach, and lung.^{7,18,20–22}

In the present study, we show that catK mRNA and protein expression is highly upregulated in advanced human atherosclerotic lesions. We further investigated the role of catK in atherosclerosis by studying mice deficient in apoE (apo^{-/-}) and catK (ie, catK^{-/-}/apoE^{-/-} mice). Here we show that a deficiency of catK not only reduces plaque progression and induces fibrosis but also affects macrophage foam cell formation.

Methods

Tissue Sampling

Atherosclerotic plaques were obtained from patients undergoing vascular surgery (Department of General Surgery, Academic Hospital, Maastricht, the Netherlands) or at autopsy (Department of Pathology, Academic Hospital Maastricht, the Netherlands). Vascular specimens were processed as described¹⁷ and classified according to Virmani et al.²³

Dot Blot Analysis

Five dot blots containing catK cDNA (≈20 ng per spot) were hybridized at high stringency with ³²P-labeled (High Prime, Boehringer Mannheim) SMART cDNA derived from pooled (n=3 per group) whole-mount human vascular plaques.¹⁷ Hybridization signals from (1) nondiseased arteries, (2) early atherosclerotic lesions, (3) advanced stable plaques, (4) lesions containing thrombus, and (5) veins were quantified by PhosphorImager analysis (Quantity One, Bio-Rad) and normalized for the signals of RNA polymerase II and human genomic DNA.

Reverse Transcription–Polymerase Chain Reaction

RNA was isolated from individual samples of veins (n=5), nondiseased arteries (n=4), early atherosclerotic plaques (n=5), advanced lesions (n=10), and lesions with thrombi (n=10), and reverse transcriptase–polymerase chain reaction (RT-PCR) was performed for catK and glyceraldehyde 3-phosphate dehydrogenase.

Western Blot Analysis

Blots were incubated with mouse monoclonal anti-catK antibody (5 μg/mL, Calbiochem) or phosphate-buffered saline, and horseradish peroxidase–coupled rabbit anti-mouse antibody (1:1000, Dako). Specific antibody binding was visualized by enhanced chemiluminescence (Amersham Pharmacia Biotech).

Animals

ApoE^{-/-} mice on a C57BL6 background were obtained from Iffa Credo (Lyon, France) and backcrossed 5 to 7 times to catK^{-/-} mice (C57BL6 background; P. Saftig). During the experimental period, mice were fed a normal chow diet. At the age of 26 weeks, male catK^{-/-}/apoE^{-/-} (n=7), apoE^{-/-} (n=8), and catK^{-/-} (n=8) mice were humanely killed after an 8-hour fast. Blood was obtained, and after in situ perfusion-fixation, the complete arterial tree was excised and fixed as described previously.²⁴ The aortic arch including its main branch points (brachiocephalic trunk, right and left common carotid arteries, and left subclavian artery) were embedded longitudinally and cut into ≈40 sections. A series of twenty 4-μm sections, which represented the central area of the arch with an intact morphology of the complete arch including branch points, was analyzed as described previously.²⁴

Lipid Profile

For assessment of lipid profiles, standard enzymatic techniques, automated on a Cobas Fara centrifugal analyzer (Hoffmann–La Roche), were used (kit Nos. 0736635, 543004, and 0148270, Hoffmann–La Roche; and kit No. 337-40A/337-10B; Sigma Chemical Co).

Evaluation of Possible Systemic Effects

More than 20 organs were excised from 4 mice per group and analyzed by microscopy of 4-μm sections stained with hematoxylin and eosin. Fluorescence-activated cell sorting (FACS) analysis of lymph nodes, blood, and spleen was performed as described previously.²⁵

Histology and Morphometry of Mouse Plaques

For histological analysis and morphometry, 4 sections (20 μm apart) were stained with hematoxylin and eosin, and 4 consecutive sections (also 20 μm apart) were stained with Lawson solution to stain the elastic laminae. Sirius red staining was performed to detect collagen. Morphometric parameters were determined as described previously.^{24,26} Atherosclerotic lesions were analyzed and classified according to Virmani et al.²³ Because the data among the initial plaque stages (intimal thickening and intimal xanthomas) and among the advanced atherosclerotic lesions (thin and thick fibrous cap atheromas and fibrocalcified plaques) were similar, data are presented for these 2 groups: initial lesions and advanced lesions.

Immunohistochemistry

(Double) immunohistochemistry was performed as described before^{24,25} with the following antibodies: anti-catK antibody (mouse monoclonal, 50 μg/mL; Calbiochem), α-smooth muscle actin monoclonal antibody (1:500, Sigma) as a marker for vascular SMCs and myofibroblasts; MAC3 rat monoclonal antibody (1:30, Pharmingen) to detect macrophages; CD3 polyclonal antibody (A0452, 1:200; Dako) to detect T lymphocytes; and CD36²⁷ and scavenger receptor (SR)-A antibodies (chicken and rabbit polyclonals; kind gifts of Prof de Beer and Prof A. Daugherty, University of Kentucky, Lexington) to determine SR immunoreactivity.

Bone Density Measurements

Trabecular mineral density (mg/cm³), total bone area (mm²), cortical mineral density (mg/cm³), and cortical thickness (mm) of the left femur were assessed in cross section by peripheral quantitative computed tomography (model XCT-960A, Norland Stratec) with a voxel size of 0.08 mm and a threshold of 0.464.

BM-Derived Macrophages

Bone marrow (BM) was flushed from the femurs and tibiae of 20- to 25-week-old apoE^{-/-} and catK^{-/-}/apoE^{-/-} mice and cultured for 8 days in RPMI medium containing L-glutamine, HEPES, 10% fetal calf serum, and 100 IU/mL penicillin/streptomycin with the addition of 15% L929 cell-conditioned medium to induce differentiation into macrophages.²⁸

Migration Assay

To determine transmigration of BM-derived macrophages, BD BioCoat Matrigel invasion chambers (BD Biosciences), serving as a reconstituted basement membrane in vitro, were used. The transmigration assay was carried out at 37°C for 24 hours (with monocyte chemoattractant protein) followed by toluidine blue staining. Ten microscopic fields were randomly chosen to count transmigrated cells.

Trypan Blue Exclusion Test

To determine the viability of both apoE^{-/-} and catK^{-/-}/apoE^{-/-} BM-derived macrophages, a trypan blue exclusion test was performed. After incubation with or without oxidized (ox) LDL for 24 hours, vital and nonvital (trypan blue–colored) cells were counted in 10 microscopic fields per sample.

LDL Extraction and Oxidation and Uptake of oxLDL

LDL was extracted from fresh human plasma by graded ultracentrifugation. The LDL was oxidized by overnight incubation at 37°C with CuSO₄. oxLDL was labeled with the fluorescent lipid 1,1'-dioctadecyl-3,3,3',3'-tetramethylindocarbocyanine perchlorate (DiI; Molecular Probes). BM-derived macrophages were incubated with 25 µg/mL DiI-labeled oxLDL for 0.5, 1, or 3 hours. The SR inhibitor poly(I)lysine (20 µg/mL) was added 5 minutes before the DiI-labeled oxLDL incubation. OxLDL uptake was determined by FACS (BD Biosciences).

High-Performance Thin-Layer Chromatography

To determine the composition of lipid storage by BM-derived macrophages, high-performance thin-layer chromatography (HPTLC) was performed. Cells were incubated with 25 µg/mL oxLDL for 24 or 48 hours. Cellular lipid accumulation per milligram protein was analyzed by HPTLC. Cholesterol acetate in chloroform (20 µg/mL) was used as an external standard.

Quantitative Real-Time PCR for SR-A and CD36

RNAs from aortic arches of 26-week-old catK^{-/-}/apoE^{-/-} mice (n=11) and apoE^{-/-} mice (n=11) were used for real-time PCR analysis. cDNA was diluted to a concentration of 2 ng/µL. The Bio-Rad MyIQ single-color real-time PCR detection system with Optic system software version 1.0 was used for real-time PCR. For each PCR, 10 ng cDNA, 2× universal PCR master mix, 300 nmol/L forward primer, 300 nmol/L backward primer, and 200 nmol/L Taqman probe were added to a final volume of 25 µL. PCR amplification of the housekeeping gene cyclophilin and of SR-A and CD36 was performed according to standard procedures (1 cycle at 50°C for 2 minutes, 1 cycle at 95°C for 10 minutes, followed by 50 cycles of 95°C for 15 seconds and 60°C for 1 minute). A standard curve was generated for all experiments, and all assays were performed in duplicate. Relative RNA copy numbers were calculated from standard curves that were obtained by serial dilution of quantified template cDNA. The expression of each target gene was normalized to the expression of the housekeeping gene cyclophilin.

Electron Microscopy

For analysis of lysosomal compartments, BM-derived macrophages were incubated with 25 µg/mL oxLDL for 24 hours at 37°C (5%

CO₂), fixed in 2.5% glutaraldehyde, embedded in 10% gelatin blocks, postfixed in 1% OsO₄ solution, dehydrated, and embedded in epoxy resin. Ultrathin sections were mounted on Formvar (1595 E, Merck)-coated 75-mesh copper grids and counterstained with uranyl acetate and lead citrate before analysis in a Philips CM100 transmission electron microscope. Ten electron microscopic fields for each condition were measured. Individual lysosomal area was determined with ImageJ software (<http://rsb.info.nih.gov/ij/>).

Statistical Analysis

When n<30, groups were compared by the nonparametric Mann-Whitney *U* test. In this case, data are expressed as means and interquartile ranges. When n>30, a parametric Student *t* test was performed, and data are expressed as mean±SEM. Data were considered statistically significant at *P*<0.05.

Results

catK mRNA Expression During Human Atherogenesis

catK mRNA is expressed at a low level in human veins, nondiseased arteries, and early atherosclerotic lesions (Figure 1A). Expression was upregulated by 28-fold in advanced but stable lesions when compared with early lesions and by 11-fold when compared with lesions containing thrombus. In addition, RT-PCR analysis of individual samples revealed no detectable catK expression in veins and nondiseased arteries, whereas 20% of early lesions, 70% of advanced lesions, and 30% of lesions containing a thrombus tested positive (Figure 1B).

catK Protein Expression

In lysates from individual early lesions, advanced stable lesions, and advanced lesions containing a thrombus (n=3 per group), at least 3 catK protein products were distinguished: the pre-proenzyme of 40 kDa, a proenzyme of 37 kDa, and the mature enzyme with a molecular weight of 27 kDa. Expression of mature catK was upregulated by >50-fold in stable lesions when compared with early lesions and by 6.5-fold when compared with lesions containing a throm-

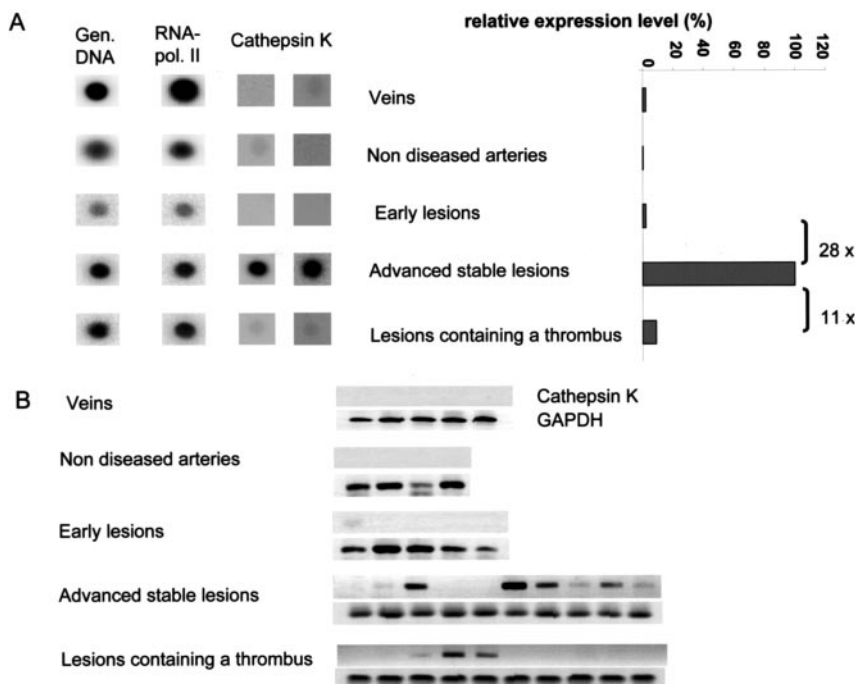


Figure 1. catK mRNA expression in different stages of plaque development. A, Two sets of 5 identical dot blots containing catK cDNA were hybridized to pools of ³²P-labeled cDNA derived from human veins, nondiseased arteries, early lesions, advanced stable lesions, and lesions with thrombus. Expression levels were normalized to the hybridization signals for genomic (Gen.) DNA and RNA polymerase (pol.) II. B, RT-PCR analysis of mRNA isolated from veins, nondiseased arteries, early lesions, advanced stable lesions, and lesions containing thrombus. GAPDH indicates glyceraldehyde 3-phosphate dehydrogenase.

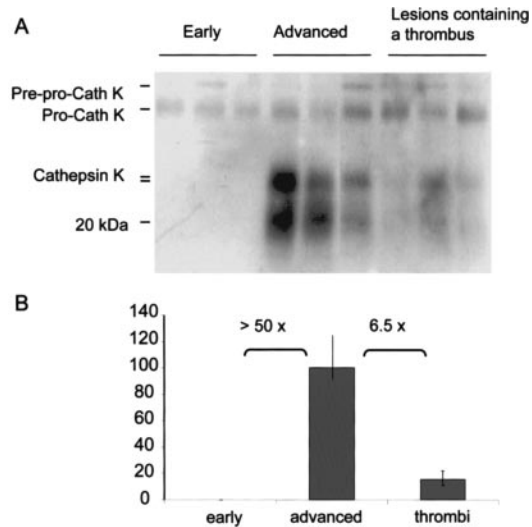


Figure 2. Western blot analysis of catK expression in human atherosclerotic lesions. A, Lanes 1 through 3, early lesions; lanes 4 through 6, advanced but stable atherosclerotic lesions; and lanes 7 through 9, lesions containing thrombus. B, Quantification of mature catK content, as judged by densitometric scanning. Cath indicates cathepsin.

bus (Figure 2B). In addition, we observed a >50-fold increase in the expression level of an ≈ 20 -kDa immunoreactive band, presumably representing a catK degradation product, in stable lesions when compared with early lesions and a 4.5-fold increase when compared with lesions with a thrombus.

In atherosclerotic plaques, catK was expressed in SMCs, macrophages, and endothelial cells (Figure 3A through 3C). In human veins, nondiseased arteries, and early atherosclerotic lesions (Figure 4A), catK expression was low. However, strong immunoreactivity was present in stable lesions (Figure 4B). The fibrous cap, shoulder region, and rim of the lipid core particularly showed high levels of catK protein immunoreactivity. Lesions containing a thrombus revealed intermediate levels of immunoreactivity, with a pattern similar to that observed in advanced stable lesions (Figure 4C). catK protein was also expressed at the actual site of plaque rupture (Figure 4D). Advanced lesions in apoE^{-/-} mice showed high levels of catK expression in the cytoplasm of vascular endothelial cells,

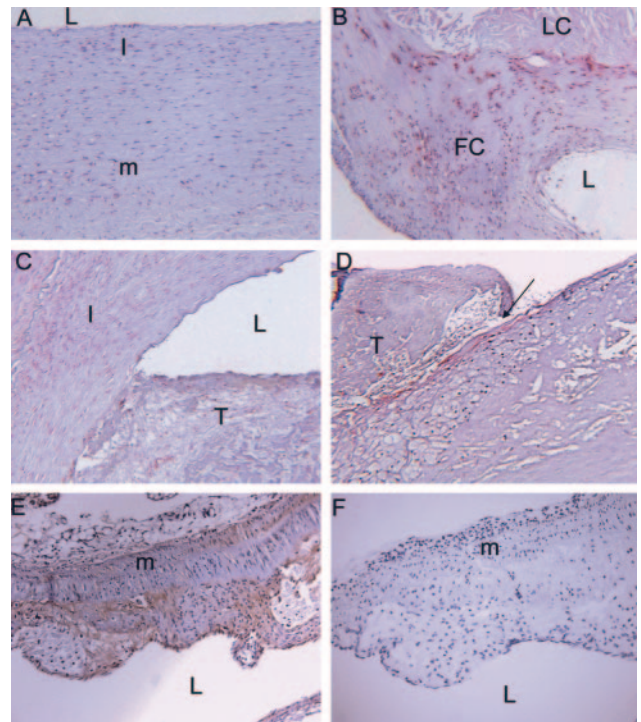


Figure 4. Localization of catK expression. Photomicrographs shows catK expression in various stages of human atherogenesis: (A) intimal xanthoma, (B) a stable plaque, (C) a lesion containing thrombus, and (D) at the actual site of plaque rupture. E shows catK expression in an advanced lesion from an apoE^{-/-} mouse, whereas F shows the absence of catK staining in a catK^{-/-} apoE^{-/-} murine advanced plaque ($\times 100$). catK immunoreactivity is depicted in red (A–D) or brown (E and F). m indicates media; I, intima; L, lumen; LC, lipid core; T, thrombus; and FC, foam cell. The arrow (D) points toward the actual site of plaque rupture.

neointimal and medial SMCs, and macrophages. As expected, catK^{-/-}/apoE^{-/-} mice showed no expression of catK (Figure 4E and 4F).

In Vivo Validation

Survival rates of catK^{-/-}/apoE^{-/-} mice, apoE^{-/-} mice, and catK^{-/-} mice were 100% in all 3 groups. Body weights were similar. Autopsy (>20 organs) revealed no macroscopic or microscopic abnormalities in sections stained with hematoxylin and eosin, except for the increased trabecularization of long

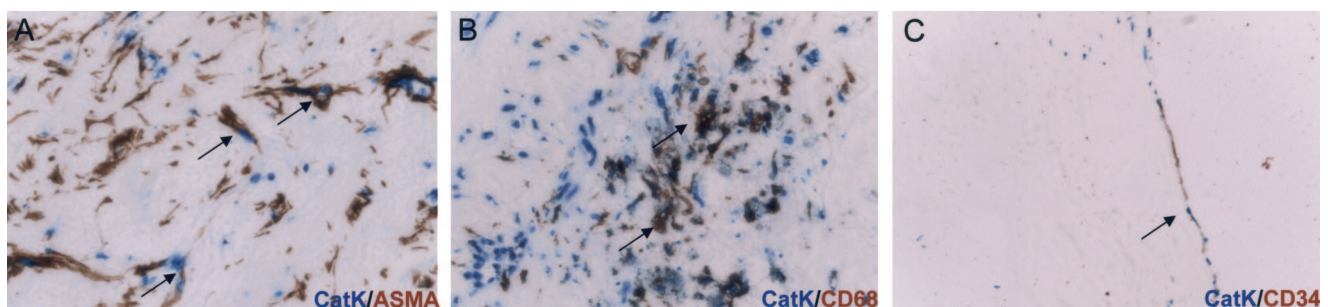


Figure 3. Cell type-specific catK expression. Double immunohistochemistry for catK (blue) and (A) α -smooth muscle actin (ASMA; brown), (B) CD68 (brown), and (C) CD34 (brown), revealing expression of catK in plaque SMCs, macrophages, and endothelial cells (arrows).

TABLE 1. Plasma Cholesterol and Triglyceride Levels

	CatK ^{-/-} /ApoE ^{-/-} (n=7)	ApoE ^{-/-} (n=8)	CatK ^{-/-} (n=8)
Total cholesterol, mg/dL	910 (596–1106)*	518 (461–1160)*	89 (47–97)*
HDL cholesterol, mg/dL	13 (10–19)*	7 (6–13)*	61 (38–66)*
LDL cholesterol, mg/dL	822 (571–1050)*	500 (445–1060)*	17 (5–29)*
Total triglyceride, mg/dL	234 (168–336)*	93 (73–387)*	51 (40–54)*
Free triglyceride, mg/dL	22 (20–27)	20 (16–25)	22 (17–23)

Values are median and (25th percentile–75th percentile).

* $P < 0.05$ for the difference between catK^{-/-} mice and both catK^{-/-}/apoE^{-/-} and apoE^{-/-} mice.

Lipid levels of catK^{-/-}/apoE^{-/-} and apoE^{-/-} mice were similar, but catK^{-/-}/apoE^{-/-} showed a trend toward higher total cholesterol ($P=0.12$), LDL cholesterol ($P=0.15$), and triglyceride ($P=0.27$) levels and lower HDL cholesterol levels ($P=0.58$).

bones in catK^{-/-} and catK^{-/-}/apoE^{-/-} mice (Data Supplement Figure; see <http://circ.ahajournals.org/cgi/content/full/CIRCULATIONAHA.105.561449/DC1>) when compared with apoE^{-/-} mice, as previously described.²⁹ The observed increase in bone trabecularization was further substantiated by bone density measurements, showing a 2-fold increase in trabecular bone density in catK^{-/-} and catK^{-/-}/apoE^{-/-} mice when compared with apoE^{-/-} mice (Data Supplement Table).

FACS analysis revealed no differences in the amount of CD3-positive cells (T cells), in the activation status of T cells between the groups (CD4 to CD8 ratio, CD25+ T cells), and the amount of GR-1-positive cells (macrophages) in lymph nodes, blood, and spleen, confirming the absence of extensive systemic effects of catK deficiency on T-cell number and activation or macrophage number (data not shown).

Although there was a trend toward higher total cholesterol, LDL, and triglyceride levels and lower HDL levels in catK^{-/-}/apoE^{-/-} mice compared with apoE^{-/-} mice, these changes were not significant (Table 1).

Plaque Burden

catK^{-/-}/apoE^{-/-} mice showed a 41.8% reduction in total plaque area (515.271 μm^2 /arch [range, 275.744 to 921.135] in catK^{-/-}/apoE^{-/-} mice versus 961.364 μm^2 /arch [range,

772.499 to 1245.254] in apoE^{-/-} mice, $P < 0.05$), whereas the total number of plaques per aortic arch did not differ (6 [range, 5 to 7] in catK^{-/-}/apoE^{-/-} mice versus 5 [range, 5 to 8] in apoE^{-/-} mice, $P < 0.05$). The decrease in total plaque area was due to a decrease in the number of advanced atherosclerotic plaques (catK^{-/-}/apoE^{-/-}: 2 [range, 2 to 4] versus apoE^{-/-}: 4 [range, 3 to 5]; $P < 0.05$; Figures 5A, 6A, and 6B). In addition, advanced plaques of catK^{-/-}/apoE^{-/-} mice were significantly smaller (Figure 5B), whereas the number of initial plaques was increased (Figure 5A). This finding indicates an important role for catK in atherosclerotic plaque progression.

Plaque Composition

In addition to the decrease in plaque progression and plaque area, significant differences in plaque composition between catK^{-/-}/apoE^{-/-} and apoE^{-/-} mice were observed. As expected, a deficiency of catK had a profound effect on plaque extracellular matrix content. Collagen content increased significantly in advanced plaques of catK^{-/-}/apoE^{-/-} mice (38.3% [range, 32.5% to 44.3%] versus 32.5% [range, 24.1% to 38.2%]; $P < 0.05$; Figures 5C, 6C, and 6D). The number of elastin breaks in the media underlying the atherosclerotic plaque was decreased in the advanced lesions of catK^{-/-}/apoE^{-/-} mice (initial lesions in catK^{-/-}/apoE^{-/-}: 1 [range, 1–1] versus in apoE^{-/-}: 1 [range, 0 to 1]; advanced lesions in catK^{-/-}/apoE^{-/-}: 1 [range, 0 to 2] versus in apoE^{-/-}: 2 [range, 0 to 3]; $P < 0.05$; Figure 6E and 6F). The relative plaque macrophage content showed a borderline significant decrease (Table 2; initial lesions, $P=0.067$; advanced lesions, $P=0.092$) in plaques of catK^{-/-}/apoE^{-/-} mice. Interestingly, individual macrophage foam cells in the plaques were increased in size (initial lesions in catK^{-/-}/apoE^{-/-}: $398.2 \pm 16.2 \mu\text{m}^2$ /foam cell versus in apoE^{-/-}: $221.7 \pm 8.7 \mu\text{m}^2$ /foam cell; advanced lesions in catK^{-/-}/apoE^{-/-}: $365.6 \pm 29.4 \mu\text{m}^2$ /foam cell versus in apoE^{-/-}: $212.7 \pm 15.1 \mu\text{m}^2$ /foam cell; $P < 0.05$; determined in all lesions of all mice included), suggesting a role for catK in foam cell formation (Figures 5D, 6G, and 6H).

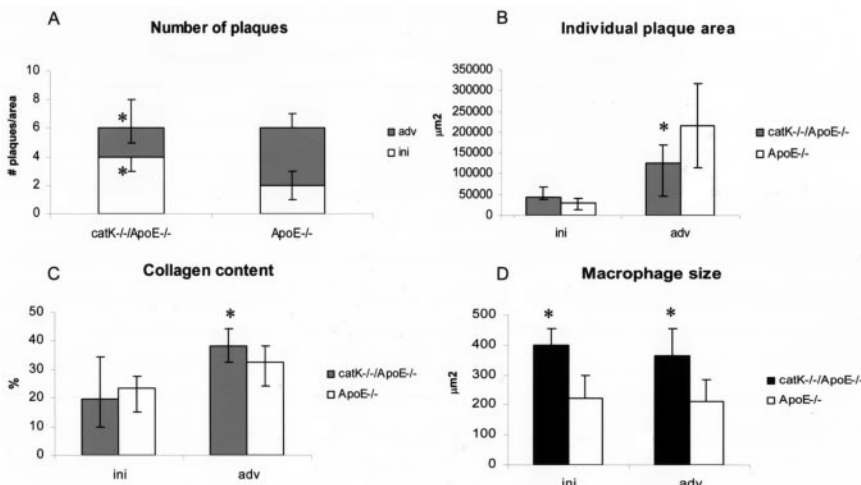


Figure 5. Box-and-whisker plots, showing quantification of plaque characteristics of catK^{-/-}/apoE^{-/-} and apoE^{-/-} mice. Number of plaques per aortic arch (A), individual plaque area (B), collagen content (C), and individual macrophage size (D) of initial (ini) and advanced (adv) lesions of catK^{-/-}/apoE^{-/-} and apoE^{-/-} mice are shown. Values are median and interquartile ranges.

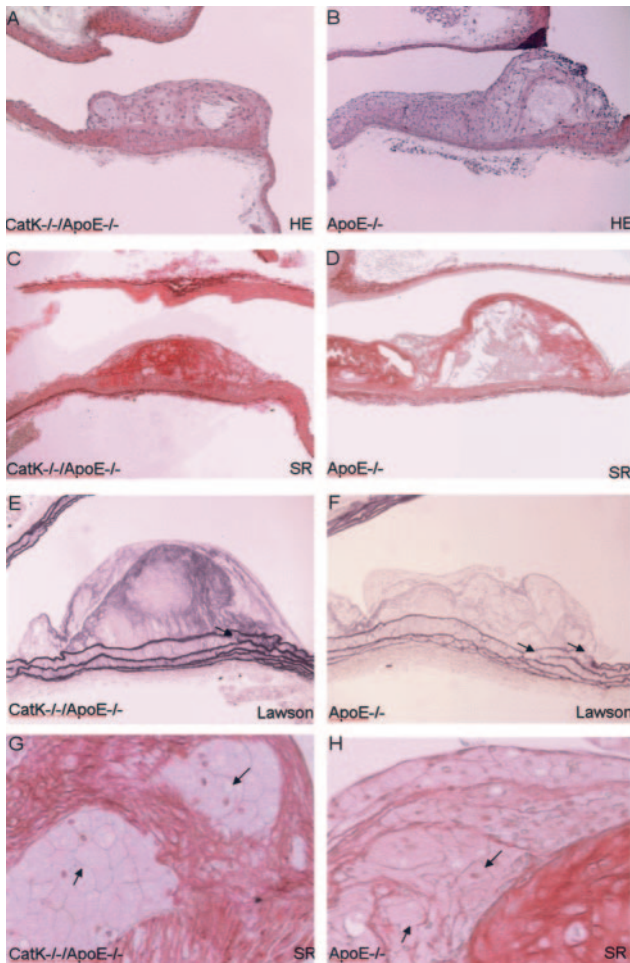


Figure 6. Histological characteristics of atherosclerotic plaques from *catK*^{-/-}/*apoE*^{-/-} and *apoE*^{-/-} mice. Hematoxylin and eosin (A and B) staining ($\times 100$) reveals a decreased advanced plaque area in *catK*^{-/-}/*apoE*^{-/-} mice. Sirius red (C and D) staining ($\times 100\times$) shows increased collagen content in plaques from *catK*^{-/-}/*apoE*^{-/-} mice. Lawson staining (E and F) shows extensive disruption of medial elastin fibers in *apoE*^{-/-} mice (arrows), which hardly occurs in *catK*^{-/-}/*apoE*^{-/-} mice. SR staining (G and H; $\times 400$) shows larger plaque macrophage foam cells (arrows) in lesions from *catK*^{-/-}/*apoE*^{-/-} mice.

T-lymphocyte content and lipid core area showed no significant differences in both initial and advanced lesions between *catK*^{-/-}/*apoE*^{-/-} and *apoE*^{-/-} mice (see Table 2).

Migration Assay

Transmigration of BM-derived macrophages was tested in a Matrigel matrix assay. In both groups, large numbers of cells transmigrated (88% to 90%), without any differences noted between *apoE*^{-/-} and *catK*^{-/-}/*apoE*^{-/-} BM-derived macrophages ($P > 0.05$). The trypan blue exclusion test showed no difference in cell death after 24 hours of oxLDL incubation between the groups ($P > 0.05$).

Mechanisms of Foam Cell Formation: In Vitro Studies

Because disruption of the *catK* gene resulted in an increase of macrophage size in atherosclerotic lesions of *catK*^{-/-}/*apoE*^{-/-}

TABLE 2. Cell Types and Characteristics

	<i>ApoE</i> ^{-/-}	<i>CatK</i> ^{-/-} / <i>ApoE</i> ^{-/-}
T-lymphocyte content (%), initial lesions	0.0 (0–0.2)	1.0 (0–2.5)
T-lymphocyte content (%), advanced lesions	0.0 (0.0–0.6)	0.8 (0.3–1.4)
Macrophage content (%), initial lesions	68.4 (65.3–77.1)	56.3 (46.1–74.1)
Macrophage content (%), advanced lesions	52.3 (39.0–56.9)	42.9 (31.2–59.1)
Lipid core area (%), advanced lesions	24.9 (17.0–31.2)	29.0 (21.4–32.3)

Values are medians and interquartile ranges.

mice, macrophage size, lysosomal area, oxLDL uptake, and subsequent storage of cholesterol esters were quantified in BM-derived macrophage foam cells in culture.

As our *in vivo* atherosclerosis data have already shown, macrophage area (as determined by DiI-oxLDL-positive staining) *in vitro* increased significantly (300%) in the absence of *catK* after 24 hours of incubation with oxLDL (Figure 7A and 7B). Furthermore, FACS analysis revealed increased uptake of DiI-labeled oxLDL in BM-derived macrophages in the absence of *catK* after 0.5, 1.0, and 3.0 hours ($P = 0.0286$ at all 3 time points; Figure 7C). Poly(I)lysine, an SR inhibitor, reduced oxLDL uptake by 76% to 80% at 3.0 hours in both groups (Figure 7C), indicating that the increased oxLDL uptake was SR mediated. To investigate which SRs were responsible for the enhanced foam cell formation in *catK*^{-/-}/*apoE*^{-/-} mice, immunohistochemistry and real-time PCR analysis for SR-A and CD36 were performed. Interestingly, both mRNA expression and immunoreactivity for SR-A did not differ between plaque macrophages of *catK*^{-/-}/*apoE*^{-/-} and *apoE*^{-/-} mice (Figure 8). However, CD36 mRNA and protein expression was significantly increased in plaques lacking *catK* (Figure 8), indicating that CD36 is one of the SRs responsible for the increased foam cell formation in the absence of *catK*.

HPTLC revealed that *catK*^{-/-}/*apoE*^{-/-} BM-derived macrophages incubated for 24 hours with oxLDL showed a 53.7% ($P = 0.004$) increase in cholesterol ester levels compared with *apoE*^{-/-} BM-derived macrophages (Figure 7D). No significant differences were seen in free cholesterol levels (data not shown).

Electron microscopy revealed an increase in lysosomal area in macrophages ($n = 10$) in the absence of *catK* (mean lysosomal size of $n > 1000$ lysosomes in *catK*^{-/-}/*apoE*^{-/-} mice: $0.44 \pm 0.02 \mu\text{m}^2$ versus in *apoE*^{-/-}: $0.23 \pm 0.01 \mu\text{m}^2$ after 24-hour incubation with oxLDL; Figure 7E).

These data illustrate the increased SR-mediated uptake of oxLDL, predominantly by CD36, in *catK*^{-/-}/*apoE*^{-/-} BM-derived macrophages, which results in increased storage of cholesterol esters in large lysosomal compartments.

Discussion

In the present study, we have shown that *catK* mRNA and protein are predominantly expressed in advanced atherosclerosis and that *catK* is involved in plaque progression. The elevated levels of *catK* mRNA and protein in stable human lesions are in agreement with the observation of Sukhova et al.,⁷ who reported high levels of *catK* in human atheromata. Moreover, other

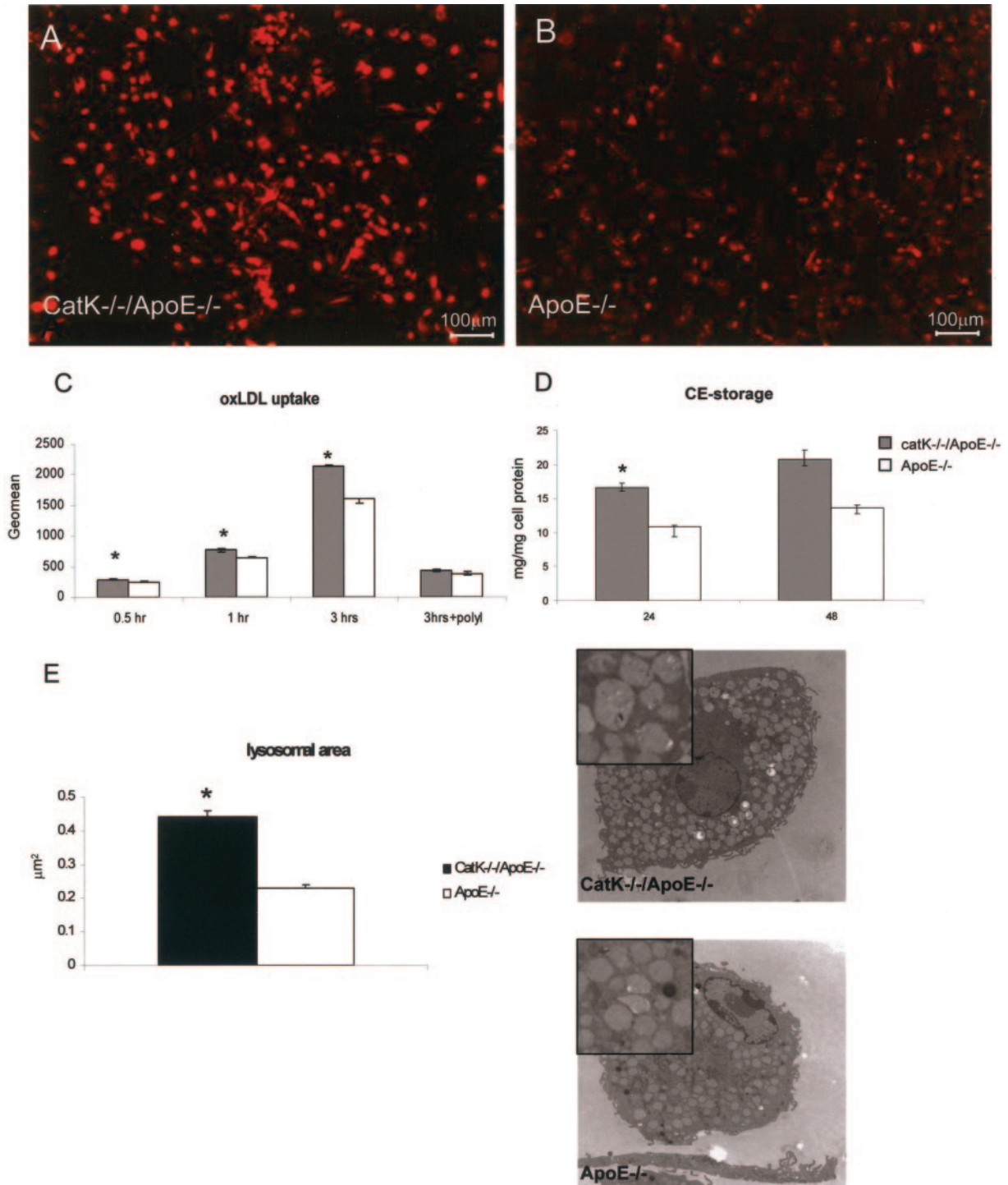


Figure 7. Uptake of Dil-labeled oxLDL (25 $\mu\text{g}/\text{mL}$) by BM-derived macrophages. A and B, Increased Dil-labeled oxLDL uptake after a 3-hour incubation in catK^{-/-}/apoE^{-/-} macrophages compared with apoE^{-/-} BM-derived macrophages. C, Increased Dil-oxLDL uptake in catK^{-/-}/apoE^{-/-} vs apoE^{-/-} bone marrow macrophages after 0.5, 1.0, and 3.0 hours of incubation ($P=0.0286$). Addition of poly(l)lysine (20 $\mu\text{g}/\text{mL}$) reduced oxLDL uptake by 76% to 80% in both groups. D, catK^{-/-}/apoE^{-/-} macrophages that were incubated for 24 hours ($n=6$) with oxLDL showed a 32% increase in cholesterol ester (CE) levels compared with apoE^{-/-} macrophages ($P=0.004$). Incubation for 48 hours ($n=3$) showed the same trend but did not reach statistical significance ($P=0.050$). E, Lysosomal area has increased in macrophages from catK^{-/-}/apoE^{-/-} mice. Note the increased lysosomal area in catK^{-/-}/apoE^{-/-} mice in the electron photomicrographs.

closely related family members of the cathepsin family, such as S, D, F, L, and V, were also found in human and mouse atherosclerotic plaques^{3,7,9,10} as well as in restenotic lesions of rabbits and rats.^{30,31} Interestingly, when compared with values in

advanced stable plaques, catK mRNA and protein levels were decreased in plaques containing a thrombus. We hypothesize that this decrease in catK levels is due to the fact that plaque rupture, ie, an event associated with high collagenolytic activity,

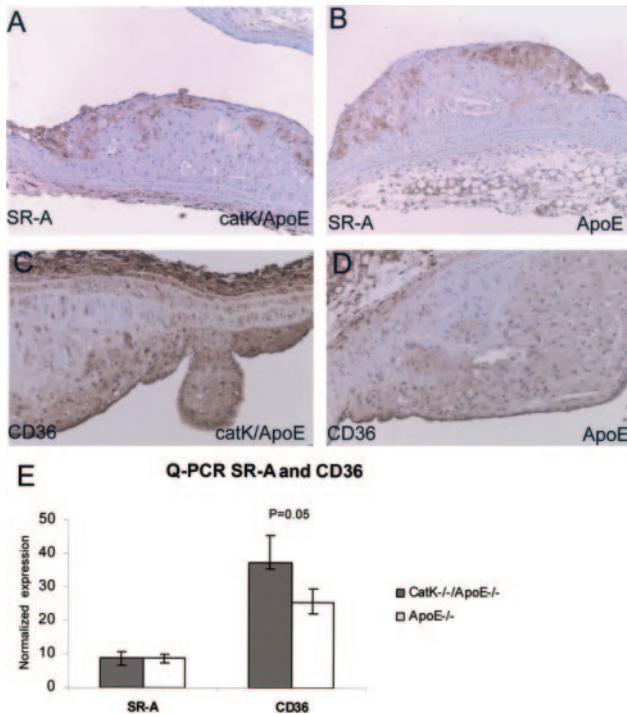


Figure 8. SR-A and CD36 expression in the absence of catK. A, B, and E, No difference in SR-A expression in atherosclerotic plaques from catK^{-/-}/apoE^{-/-} vs apoE^{-/-} mice. C, D, and E, Increased mRNA and protein expression of CD36 in plaques from catK^{-/-} mice vs apoE^{-/-} mice.

has already taken place in lesions containing an organized thrombus. Consequently, catK levels decrease. Plaques containing a thrombus are in an “active wound-healing” phase, which also requires deposition of collagen rather than extensive collagen breakdown. Because catK levels in plaques containing a thrombus are still higher compared with initial atherosclerotic lesions, we think that catK is also involved in the healing process after plaque rupture.

In advanced atherosclerotic lesions of apoE^{-/-} mice, a deficiency of catK resulted in a highly fibrotic plaque phenotype. This phenomenon was not observed in cathepsin S^{-/-}/LDL receptor^{-/-} mice.³² Although most cathepsin family members show elastolytic and some collagenolytic activity, catK is the most potent collagenase, capable of cleaving triple-helical collagens at multiple sites.^{33–35} The unique collagenolytic property of catK may explain the fibrotic phenotype observed in catK^{-/-}/apoE^{-/-} mice. The fibrotic phenotype was also observed in a model of bleomycin-induced lung fibrosis, in which catK^{-/-} mice exhibited significantly more fibrosis than did wild-type mice.²² Moreover, a deficiency of catK reduced the number of elastin breaks in the media underlying the plaque, indicating that aneurysm formation might be prevented in the absence of catK. No true plaque ruptures or intraplaque hemorrhages were observed in any of the groups.

The deficiency of catK in apoE^{-/-} mice not only affected the extracellular matrix component of atherosclerotic plaques but also had a profound effect on macrophage foam cell formation. A deficiency of catK increased the

SR-mediated uptake of oxLDL and increased storage of cholesterol esters in macrophages. Moreover, electron microscopic analysis of macrophage foam cells revealed increased lysosomal size in the absence of catK. These phenomena resulted in the large macrophage foam cells that were observed in the plaques of catK^{-/-}/apoE^{-/-} mice and in our cell culture studies. Cathepsins D and F are known inducers of foam cell formation that modify LDL, which increases macrophage LDL uptake and facilitates the binding of modified LDL to proteoglycans.⁹ However, the exact mechanism by which catK induces foam cell formation still needs to be investigated, although our data point toward an SR-mediated process with a role for CD36 in particular. Interestingly, reports on the role of CD36 in atherosclerosis are somewhat ambivalent, with some claiming a proatherogenic role for CD36 in plaque formation³⁶ whereas others do not.³⁷ However, regulation of the uptake of oxLDL of plaque macrophages is a complex process with many players,³⁸ of which the catK-SR axis might be an important one.

Cathepsins are also involved in the modulation of cholesterol efflux. At neutral pH, cathepsin F but not catK is able to partially degrade lipid-free apoA-I and partially inhibit cholesterol efflux, whereas cathepsin S is capable of completely inhibiting cholesterol efflux.³⁹ However, at pH 5 to 6, catK inhibits cholesterol efflux as well by inhibiting apoA-I-induced efflux. Therefore, it might be expected that a deficiency of catK would increase cholesterol efflux. However, because catK is only indirectly involved in the inhibition of cholesterol efflux,³⁹ this increase in cholesterol efflux might not be sufficient to compensate for the increase in foam cell formation in catK^{-/-}/apoE^{-/-} mice.

The present study shows a dual effect for catK in atherogenesis: Absence of catK induces extracellular matrix deposition and accelerates foam cell formation. From an atherosclerosis treatment perspective, these effects seem somewhat contradictory but can be explained. Cathepsins are predominantly synthesized and targeted to the acidic compartments of the cell, lysosomes and endosomes. In these compartments, pH is optimal for their activity, and it is here that cathepsins degrade unwanted intracellular or endocytosed proteins such as modified LDL. However, although cathepsins have a very narrow pH optimum (pH 4 to 6), they have also demonstrated activity in media of cultured macrophages, endothelial cells, and SMCs.^{11,15,40,41} When macrophages make contact with the extracellular matrix, a localized acidic environment is formed that allows cathepsins to degrade the extracellular matrix.⁴¹ In atherosclerotic plaques, the microenvironment is somewhat acidic owing to inflammation and hypoxia,⁴² which facilitate the actions of cathepsins. A deficiency of catK thus limits the degradation of modified LDL and at the same time, prevents degradation of the extracellular matrix, thereby inducing atherosclerotic plaques with large macrophage foam cells and profound plaque fibrosis.

Our findings on the in vivo function of catK in ApoE-deficient mice and its expression profile in human atherosclerotic lesions identify catK as a potential therapeutic target. Assuming similar effects in humans, inhibition of catK

activity could lead to decreased plaque progression and increased plaque stability. In addition, inhibition of catK activity might be beneficial in the treatment of osteoporosis, as catK deficiency, both in humans and in mice, resulted in a significant increase in trabecular bone density. However, the role of catK on foam cell formation and serum lipid levels should be taken into account. Deficiency of catK aggravates foam cell formation that may affect plaque stability. Moreover, catK^{-/-}/ApoE^{-/-} mice showed a trend toward increased serum cholesterol, LDL cholesterol, and triglyceride levels and decreased HDL levels. Therefore, combination therapy using a catK inhibitor and a lipid-lowering drug such as a HMG-CoA reductase inhibitor may be preferable.

Acknowledgments

This work was supported by the Netherlands Heart Foundation (Dr E. Lutgens; Dr E. Dekker stipend 2000T41), by the Netherlands Organization for Scientific Research (Dr Cleutjens; NWO grant 902-26-223), and by the Fonds der Chemischen Industrie and the Interuniversity Attraction Poles Program (Belgium, P5/19; to Dr Saftig). We also thank B. Jutten, H. Duimel, W. Boon, I. Middeldorp, and K. Schapira for excellent technical assistance. We further acknowledge Dr J. Peters, Organon, Oss, for bone density measurements, and Dr D. Rateri, University of Kentucky, Lexington, for generation of the SR-A antibodies.

Disclosures

Drs Sijbers, Fisher, Long, and Black are employees of Organon Research.

References

- Turk V, Turk B, Turk D. Lysosomal cysteine proteases: facts and opportunities. *EMBO J*. 2001;20:4629–4633.
- Liu J, Sukhova GK, Sun JS, Xu WH, Libby P, Shi GP. Lysosomal cysteine proteases in atherosclerosis. *Arterioscler Thromb Vasc Biol*. 2004;24:1359–1366.
- Jormsjo S, Wuttge DM, Sirsjo A, Whatling C, Hamsten A, Stemme S, Eriksson P. Differential expression of cysteine and aspartic proteases during progression of atherosclerosis in apolipoprotein E-deficient mice. *Am J Pathol*. 2002;161:939–945.
- Hiltunen MO, Tuomisto TT, Niemi M, Brasen JH, Rissanen TT, Toronen P, Vajanto I, Yla-Herttuala S. Changes in gene expression in atherosclerotic plaques analyzed using DNA array. *Atherosclerosis*. 2002;165:23–32.
- Tung WS, Lee JK, Thompson RW. Simultaneous analysis of 1176 gene products in normal human aorta and abdominal aortic aneurysms using a membrane-based complementary DNA expression array. *J Vasc Surg*. 2001;34:143–150.
- Chen J, Tung CH, Mahmood U, Ntziachristos V, Gyurko R, Fishman MC, Huang PL, Weissleder R. In vivo imaging of proteolytic activity in atherosclerosis. *Circulation*. 2002;105:2766–2771.
- Sukhova GK, Shi GP, Simon DI, Chapman HA, Libby P. Expression of the elastolytic cathepsins S and K in human atheroma and regulation of their production in smooth muscle cells. *J Clin Invest*. 1998;102:576–583.
- Hakala JK, Oksjoki R, Laine P, Du H, Grabowski GA, Kovanen PT, Pentikainen MO. Lysosomal enzymes are released from cultured human macrophages, hydrolyze LDL in vitro, and are present extracellularly in human atherosclerotic lesions. *Arterioscler Thromb Vasc Biol*. 2003;23:1430–1436.
- Oorni K, Sneek M, Bromme D, Pentikainen MO, Lindstedt KA, Mayranpaa M, Aitio H, Kovanen PT. Cysteine protease cathepsin F is expressed in human atherosclerotic lesions, is secreted by cultured macrophages, and modifies low density lipoprotein particles in vitro. *J Biol Chem*. 2004;279:34776–34784.
- Yasuda Y, Li Z, Greenbaum D, Bogoy M, Weber E, Bromme D. Cathepsin V, a novel and potent elastolytic activity expressed in activated macrophages. *J Biol Chem*. 2004;279:36761–36770.
- Sukhova GK, Zhang Y, Pan JH, Wada Y, Yamamoto T, Naito M, Kodama T, Tsimikas S, Witzum JL, Lu ML, Sakara Y, Chin MT, Libby P, Shi GP. Deficiency of cathepsin S reduces atherosclerosis in LDL receptor-deficient mice. *J Clin Invest*. 2003;111:897–906.
- Shi GP, Sukhova GK, Kuzuya M, Ye Q, Du J, Zhang Y, Pan JH, Lu ML, Cheng XW, Iguchi A, Perrey S, Lee AM, Chapman HA, Libby P. Deficiency of the cysteine protease cathepsin S impairs microvessel growth. *Circ Res*. 2003;92:493–500.
- Urbich C, Heeschen C, Aicher A, Sasaki K, Bruhl T, Farhadi MR, Vajkoczy P, Hofmann WK, Peters C, Pennacchio LA, Abolmaali ND, Chavakis E, Reinheckel T, Zeiher AM, Dimmeler S. Cathepsin L is required for endothelial progenitor cell-induced neovascularization. *Nat Med*. 2005;11:206–213.
- Barrett AJ, Davies ME, Grubb A. The place of human γ -trace (cystatin C) amongst the cysteine proteinase inhibitors. *Biochem Biophys Res Commun*. 1984;120:631–636.
- Shi GP, Sukhova GK, Grubb A, Ducharme A, Rhode LH, Lee RT, Ridker PM, Libby P, Chapman HA. Cystatin C deficiency in human atherosclerosis and aortic aneurysms. *J Clin Invest*. 1999;104:1191–1197.
- Sukhova GK, Wang B, Libby P, Pan JH, Zhang Y, Grubb A, Fang K, Chapman HA, Shi GP. Cystatin C deficiency increases elastic lamina degradation and aortic dilatation in apolipoprotein E-null mice. *Circ Res*. 2005;96:368–375.
- Faber BC, Cleutjens KB, Niessen RL, Aarts PL, Boon W, Greenberg AS, Kitslaar PJ, Tordoir JH, Daemen MJ. Identification of genes potentially involved in rupture of human atherosclerotic plaques. *Circ Res*. 2001;89:547–554.
- Bromme D, Okamoto K, Wang BB, Biroc S. Human cathepsin O2, a matrix protein-degrading cysteine protease expressed in osteoclasts: functional expression of human cathepsin O2 in *Spodoptera frugiperda* and characterization of the enzyme. *J Biol Chem*. 1996;271:2126–2132.
- Lecaille F, Choe Y, Brandt W, Li Z, Craik CS, Bromme D. Selective inhibition of the collagenolytic activity of human cathepsin K by altering its S2 subsite specificity. *Biochemistry*. 2002;41:8447–8454.
- Shi GP, Chapman HA, Bhairi SM, DeLeeuw C, Reddy VY, Weiss SJ. Molecular cloning of human cathepsin O, a novel endoproteinase and homologue of rabbit OC2. *FEBS Lett*. 1995;357:129–134.
- Buhling F, Peitz U, Kruger S, Kuster D, Vieth M, Gebert I, Roessner A, Weber E, Malfertheiner P, Wex T. Cathepsins K, L, B, X and W are differentially expressed in normal and chronically inflamed gastric mucosa. *Biol Chem*. 2004;385:439–445.
- Buhling F, Rocken C, Brasch F, Hartig R, Yasuda Y, Saftig P, Bromme D, Welte T. Pivotal role of cathepsin K in lung fibrosis. *Am J Pathol*. 2004;164:2203–2216.
- Virmani R, Kolodgie FD, Burke AP, Farb A, Schwartz SM. Lessons from sudden coronary death: a comprehensive morphological classification scheme for atherosclerotic lesions. *Arterioscler Thromb Vasc Biol*. 2000;20:1262–1275.
- Lutgens E, Gorelik L, Daemen MJ, de Muinck ED, Grewal IS, Kotliansky VE, Flavell RA. Requirement for CD154 in the progression of atherosclerosis. *Nat Med*. 1999;5:1313–1316.
- Lutgens E, Gijbels M, Smook M, Heeringa P, Gotwals P, Kotliansky VE, Daemen MJ. Transforming growth factor- β mediates balance between inflammation and fibrosis during plaque progression. *Arterioscler Thromb Vasc Biol*. 2002;22:975–982.
- Lutgens E, Daemen MJ. Transforming growth factor- β : a local or systemic mediator of plaque stability? *Circ Res*. 2001;89:853–855.
- de Villiers WJS, Cai L, Webb NR, de Beer MC, van der Westhuyzen DR, de Beer FC. CD36 does not play a direct role in HDL or LDL metabolism. *J Lipid Res*. 2001;42:1231–1238.
- Kanters E, Pasparakis M, Gijbels MJ, Vergouwe MN, Partouns-Hendriks I, Fijneman RJ, Clausen BE, Forster I, Kockx MM, Rajewsky K, Kraal G, Hofker MH, de Winther MP. Inhibition of NF- κ B activation in macrophages increases atherosclerosis in LDL receptor-deficient mice. *J Clin Invest*. 2003;112:1176–1185.
- Saftig P, Hunziker E, Wehmeyer O, Jones S, Boyde A, Rommerskirch W, Moritz JD, Schu P, von Figura K. Impaired osteoclastic bone resorption leads to osteopetrosis in cathepsin-K-deficient mice. *Proc Natl Acad Sci U S A*. 1998;95:13453–13458.
- Burns-Kurtis CL, Olzinski AR, Needle S, Fox JH, Capper EA, Kelly FM, McQueney MS, Romanic AM. Cathepsin S expression is up-regulated following balloon angioplasty in the hypercholesterolemic rabbit. *Cardiovasc Res*. 2004;62:610–620.

31. Cheng XW, Kuzuya M, Sasaki T, Arakawa K, Kanda S, Sumi D, Koike T, Maeda K, Tamaya-Mori N, Shi GP, Saito N, Iguchi A. Increased expression of elastolytic cysteine proteases, cathepsins S and K, in the neointima of balloon-injured rat carotid arteries. *Am J Pathol.* 2004;164:243–251.
32. Sukhova GK, Zhang Y, Pan JH, Wada Y, Yamamoto T, Naito M, Kodama T, Tsimikas S, Witztum JL, Lu ML, Sakara Y, Chin MT, Libby P, Shi GP. Deficiency of cathepsin S reduces atherosclerosis in LDL receptor-deficient mice. *J Clin Invest.* 2003;111:897–906.
33. Garnero P, Borel O, Byrjalsen I, Ferreras M, Drake FH, McQueney MS, Foged NT, Delmas PD, Delaisse JM. The collagenolytic activity of cathepsin K is unique among mammalian proteinases. *J Biol Chem.* 1998;273:32347–32352.
34. Kafienah W, Bromme D, Buttler DJ, Croucher LJ, Hollander AP. Human cathepsin K cleaves native type I and II collagens at the N-terminal end of the triple helix. *Biochem J.* 1998;331(pt 3):727–732.
35. Li Z, Yasuda Y, Li W, Bogyo M, Katz N, Gordon RE, Fields GB, Bromme D. Regulation of collagenase activities of human cathepsins by glycosaminoglycans. *J Biol Chem.* 2004;279:5470–5479.
36. Febbraio M, Guy E, Silverstein RL. Stem cell transplantation reveals that absence of macrophage CD36 is protective against atherosclerosis. *Arterioscler Thromb Vasc Biol.* 2004;24:2333–2338.
37. Moore KJ, Kunjathoor VV, Koehn SL, Manning JJ, Tseng AA, Silver JM, McKee M, Freeman MW. Loss of receptor-mediated lipid uptake via scavenger receptor A or CD36 pathways does not ameliorate atherosclerosis in hyperlipidemic mice. *J Clin Invest.* 2005;115:2192–201.
38. Witztum JL. You are right too! *J Clin Invest.* 2005;115:2072–2075.
39. Lindstedt L, Lee M, Oorni K, Bromme D, Kovanen PT. Cathepsins F and S block HDL3-induced cholesterol efflux from macrophage foam cells. *Biochem Biophys Res Commun.* 2003;312:1019–1024.
40. Reddy VY, Zhang QY, Weiss SJ. Pericellular mobilization of the tissue-destructive cysteine proteinases, cathepsins B, L, and S, by human monocyte-derived macrophages. *Proc Natl Acad Sci U S A.* 1995;92:3849–3853.
41. Punturieri A, Filippov S, Allen E, Caras I, Murray R, Reddy V, Weiss SJ. Regulation of elastinolytic cysteine proteinase activity in normal and cathepsin K-deficient human macrophages. *J Exp Med.* 2000;192:789–799.
42. Naghavi M, John R, Naguib S, Siadaty MS, Grasu R, Kurian KC, van Winkle WB, Soller B, Litovsky S, Madjid M, Willerson JT, Casscells W. pH heterogeneity of human and rabbit atherosclerotic plaques: a new insight into detection of vulnerable plaque. *Atherosclerosis.* 2002;164:27–35.

CLINICAL PERSPECTIVE

catK is a lysosomal cysteine protease that is highly upregulated in advanced human atherosclerotic plaques. We found that a deficiency of catK in a mouse model of atherosclerosis (catK^{-/-}/apoE^{-/-} mice) decreased the extent and progression of atherosclerosis. Moreover, in the absence of catK, atherosclerotic plaques contained more collagen and less medial elastin breakdown, features of a stable plaque phenotype. However, catK deficiency also aggravated macrophage foam cell formation. These macrophages were able to take up more oxLDL and showed an increase in cholesterol ester storage. In addition, plasma lipid levels showed a tendency to increase. Our findings on the in vivo function of catK in apoE-deficient mice and its expression profile in human atherosclerotic lesions identify catK as a potential therapeutic target. If one assumes similar effects in humans, inhibition of catK activity could lead to decreased plaque progression and increased plaque stability. In addition, inhibition of catK activity might be beneficial in the treatment of osteoporosis, because catK deficiency in both humans and mice resulted in a significant increase in trabecular bone density. However, the role of catK in foam cell formation and its effect on serum lipid levels should be taken into account. Deficiency of catK aggravates foam cell formation that may affect plaque stability. Moreover, catK^{-/-}/apoE^{-/-} mice showed a trend toward increased serum cholesterol, LDL, and triglyceride levels and decreased HDL levels. Therefore, combination therapy with a catK inhibitor and a lipid-lowering drug like a statin might be preferable.